

UDC 534.232

T.V. Makarova, PhD, Assoc.Prof.,  
A.V. Zhukova, PhD, Assoc.Prof.

Odessa National Polytechnic University, 1 Shevchenko Ave., 65044 Odessa, Ukraine; e-mail: rada@sky.od.ua

## THE INERTIAL PROPERTIES OF PULSING INTERFLOW AREA OF COUNTERFLOW HYDRODYNAMIC RADIATOR

*T.V. Makarova, A.V. Zhukova. Інерційні властивості пульсуючої міжструминної області протиточного гідродинамічного випромінювача.* Струминні гідродинамічні випромінювачі (ГДВ) представляють собою пристрої, в яких частина кінетичної енергії затопленого струменя трансформується у пульсації внутрішньої міжструминної області і коливні рухи струминної оболонки. Процес звукоутворення в ГДВ пов'язан з його конструктивних особливостей. **Мета:** Метою роботи є дослідження інерційних властивостей міжструминної пульсуючої області ГДВ з урахуванням його геометричних особливостей. **Матеріали і методи:** Для дослідження пульсуючої області запропоновано спрощену сферичну модель пульсуючої кавітуючої області струминного гідродинамічного випромінювача протиточного типу в двох модифікаціях: з урахуванням обсягу, зайнятого струменем, що витікає з сопла, і без нього. **Результати:** За результатами дослідження визначено характерні розміри і просторові обмеження для запропонованих модифікацій. Знайдено власну масу, приєднану масу і сукупну масу пульсуючої області (пульсатора). Отримано залежності відповідних масових співвідношень від радіуса пульсатора. **Висновки:** Показано, що переважну роль у сукупній масі відіграє саме приєднана маса, яка майже в 6 разів більша за власну масу пульсатора. Врахування центрального осевого каналу, зайнятого струменем з сопла, збільшує вклад приєднаної маси в сукупну масу пульсатора. Вплив приєднаної маси посилюється при збільшенні газомісту двофазного середовища, тобто при розвитку кавітації. Сукупні маси пульсуючої ділянки в різних модифікаціях моделі близькі між собою через взаємну компенсацію двох факторів — зростання приєднаної маси пульсатора і зменшення його власної маси при порівняно малих обсягах сфери.

*Ключові слова:* гідродинамічний випромінювач, міжструминна область, приєднана маса.

*T.V. Makarova, A.V. Zhukova. The inertial properties of pulsing interflow area of counterflow hydrodynamic radiator.* The jet hydrodynamic radiators (HDR) are the devices where part of kinetic energy of flooded jet is transformed to pulsations of internal interflow area and flow shell fluctuations. The sound generation process in HDR is involved with its constructional features. **Aim:** The aim of this work is to study the inertial properties of the HDR pulsating interflow area taking into account its geometric singularities. **Materials and Methods:** It was proposed to study the pulsating area using the simplified sphere model of pulsating cavitating area of the counterflow type jet hydrodynamic radiator. This radiator can be implemented in two modifications: taking into account the volume that occupies by jet from the nozzle with and without accounting of it. **Results:** The characteristic dimensions and spatial restrictions are determined for the mentioned modifications based on the research results. The own mass, apparent mass and total mass of pulsating area (pulsator) were determined. The dependencies of the corresponding mass relations versus pulsator radius were obtained. **Conclusions:** It was shown that specifically apparent mass has dominance in total one and it is almost 6 times greater than pulsator own mass. The consideration of the central axial passage occupied by jet out of muzzle increases the contribution of apparent mass to total mass. The influence of apparent mass intensifies under increase of the gas content of dual-phase environment, i.e. under cavitation propagation. The total masses of pulsating area are nearest one to another in various models modifications due to cancellation effect of two factors — increase of pulsator apparent mass and decrease of its own mass under comparatively low sphere volume.

*Keywords:* hydrodynamic radiator, interflow area, apparent mass.

**Introduction.** The jet hydrodynamic radiators (HDR) are the devices where part of kinetic energy of submerged flow is transformed to pulsations of internal interflow area and flow shell fluctuations. The HDR inner area embodies an intensive cavitation zone generated within a toroidal vortex between the nozzle and the obstacle, and consists of steam-and-gas bubbles (cavities) mixture at the liquid, thus representing a biphasic medium. The interflow area pulsation excites the natural frequency vibrations at flooded shell that leads to the high intensity tonal acoustic signal. Just when the interflow pulsations field frequency is the same as the frequency of the flow shell fluctuations' fundamental harmonic there arises a maximum acoustic signal corresponding to the optimal mode of HDR operation.

The process of sound generation with HDR issues from the emitter's design features, giving rise to an interaction between its operating area main elements: effluent and reflected flows, as well as the biphasic interflow area. This zone can be considered as a single energetically coherent hydrodynamic system.

DOI 10.15276/opu.3.47.2015.16

© 2015 The Authors. This is an open access article under the CC BY license (<http://creativecommons.org/licenses/by/4.0/>).

The source [1] suggested that the emitter's operating area forms a resonant system consisting of the inner elastic cavitation medium, the flow shell properly and the external apparent mass. Thus, proposed is one of possible mechanisms for sound generation with HDR. Some authors, e.g. [2], studied transversal oscillations of submerged annular flow shells. In addition, based on the mechanism presented at [1], there were identified the HDR sound field characteristics and explained several effects observed in experimental studies [3]. In particular, the use of two-phase medium density data [4] allowed the evaluation of such medium elastic properties and of the passing-through sound's speed. However, a complete description of the HDR-sound generating mechanism apart of flow shells' models, requires a more complete and systematic theoretical research as to the interflow pulsing area (pulsator). This area should be considered as a whole pulsating volume oscillating in a liquid medium, taking into account its inertial (mass) and elastic properties. The first step in solving this problem is to define the integral characteristic i.e. the total pulsator mass.

**The aim** of this work is to study the inertial properties of the HDR pulsating interflow area taking into account its geometric singularities. Finding the pulsator mass involves two tasks. Firstly, we proceed to its proper weight estimation, based on the internal volume contents. Second step refers to finding the apparent mass, which allows to take into account the reactive mass resistance of the pulsator-surrounding environment. Also necessary is to estimate these components' contribution into the resulting total mass of the pulsator.

**Materials and Methods.** The pulsing interflow area at the studied counterflow HDRs functioning under advanced cavitation mode represents a complex dynamic group of vapor-gas cavities suspended in a liquid. This complex group is characterized by a number of parameters determining the ratio in volume of the liquid and vapor-gas phases, and hence its weight. An additional factor is the pulsator total mass (as well as of both its components') general dependence onto the particular configuration of a model selected for studying. The model characteristics include not only a set of its own geometrical parameters, but the parameters of its limiting flow shell enveloping the simulated object (pulsator). Therefore, a special attention should be given to the peculiar features of the object – to – environment boundaries.

Thus, while researching the HDR as a source of acoustic emission, first stage task involves the choice of an adequate pulsator model; the second one includes its inertial characteristics study, i.e. determination of the total mass, represented by both components. Also of interest is to compare the total mass and its components values at different models and their modifications due to hydrodynamic conditions in the acoustic area generated by the HDR under study.

The counterflow HDR model can be represented as follows. The coaxial nozzle 1 and deflector 2 are submerged in the working fluid (Fig. 1). A circular jet flows out of the nozzle, and turns into an enveloping flow 3 in the form of a truncated cone by means of the reflector's parabolic concavity 4. The nozzle's outer edge receiving the incident flow represent a truncated cone. As a result of asymmetrical incidence on the obstacle the flow becomes transversally instable and may bifurcate. At that a part of the liquid flows out into the outer (with respect to the emitter) space, and the other part arrives in the interior one, where folds into a toroidal vortex 5. Inside that vortex the cavitation occurs due to the Bernoulli effect, and creates a biphasic medium consisting of liquid and vapor-gas bubbles (cavities). Periodically accumulated the inner areas' content exerts pressure on the flow shell which thereby is forced to diverge and busts into outer environment. Obviously, the internal cavitation zone (non-uniform and non-stationary) content produces a significant impact on the nature of flow shell transverse vibrations arising, as several proper dynamic nonequilibrium processes can occur inside of such cavitation zone. The cavitation zone geometrical parameters and hence the HDR operation mode vary depending on the distance between the nozzle and the deflector.

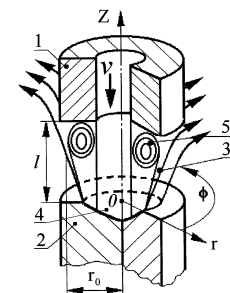


Fig. 1. HDR model: 1 — nozzle; 2 — deflector; 3 — flooded flow shell; 4 — parabolic concavity; 5 — toroid vortex

To investigate the pulsing area suggested is the most simple model of a pulsing sphere with radius  $R_p$ , encircled at the HDR interflow area space. The model is considered in two versions: without taking into account the volume occupied by the central flooded jet flow from the HDR nozzle (Fig. 2, *a*) and a model forming a sphere with a “cut” axial cylindrical channel occupied by the jet and therefore not included to the pulsator’s considered volume (Fig. 2, *b*). Thus the problem is reduced to an analysis of principle and mechanism for determining the pulsator total mass in both cases, as well as the comparative analysis of the proposed model modifications using the results obtained.

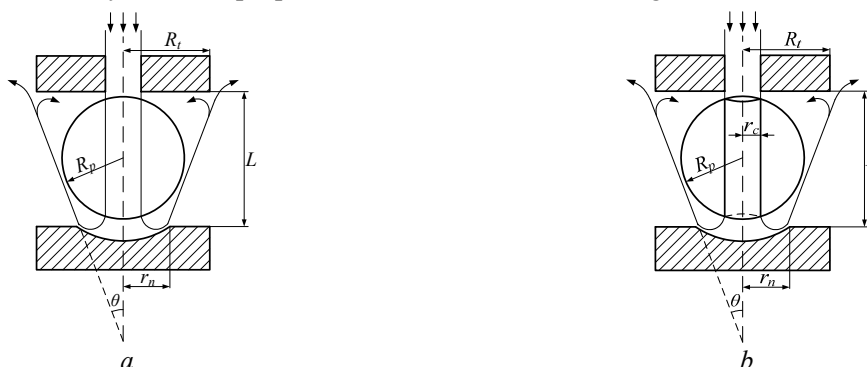


Fig. 2. Interflow pulsing area model of counterflow HDR:  
*a* —excluding the central axial channel locating the flow; *b* —including the central axial channel

We take the following HDR interflow area’s and pulsing area’s basic geometric parameters:

$L$  —distance between the nozzle 1, releasing a jet of working fluid, and the deflector 2, forming the submerged flow shell;

$r_c$  —nozzle’s inner radius (central jet);

$R_t$  —nozzle’s outer radius;

$r_n$  —deflector’s parabolic concavity 4 radius;

$\theta$  —submerged flow shell 3 cone’s opening angle.

Before proceeding to determine the pulsator mass, necessary is to estimate the model’s characteristic dimensions. The  $R_p$  sphere equilibrium radius should be such that it fits into the space within by the submerged flow shell boundaries, as shown in Fig. 2, *a*. This means the relevance of the following conditions limiting the pulsator radius:

— Firstly, it is obvious that the sphere should be placed between the nozzle and the deflector, i.e.

$$R_p < \frac{1}{2}L.$$

— Secondly, directly the model geometry is immediately implying the two expressions relating the pulsator’s model geometric parameters with these of the HDR interflow area, i.e. imposing also this area’s spatial constraints:

$$R_p < \frac{L \operatorname{tg} \theta + r_n}{1 + \operatorname{tg} \theta}, \quad (1)$$

$$R_p < \frac{R_t}{1 + \operatorname{tg} \theta}. \quad (2)$$

The difference between the nozzle outer radius and the deflector’s concavity radius being of the same order as the distance between the nozzle and the deflector, i.e.  $R_t - r_n \approx L$  and thus  $\operatorname{tg} \theta = 1$  the obtained conditions are the same.

We accept the pulsator own weight  $M_c$  as the mass of its content enveloped with its volume. The apparent mass  $M_a$  allows to take into account the existence of pulsator-surrounding environment. Then the model of a spherical area under volumetric fluctuations in a liquid medium, its total mass  $M$  shall represent the sum of its own and apparent masses:

$$M = M_c + M_a. \quad (3)$$

Under advanced cavitation mode the pulsing area content consists of liquid mixed with the steam and gas inclusions, so the pulsing area own mass includes two corresponding components :

$$M_c^{(1)} = (1 - \eta)V_p^{(1)}\rho_l + \eta V_p^{(1)}\rho_g, \quad (4)$$

where  $M_c^{(1)}$  — pulsator's own mass at the first modification of spheric model;

$V_p^{(1)}$  — pulsator's volume;

$\eta$  — volumetric gas content;

$\rho_l$  — working fluid density;

$\rho_g$  — gas density.

Considering the volumetric proportion of liquid-to-gas at biphasic this one of comparable values and with respect to the fact of gas density being essentially lower that this one of the liquid, we get from (4) the own mass describing expression:

$$M_c^{(1)} \approx (1 - \eta)V_p^{(1)}\rho_l = (1 - \eta)M_l^{sph}, \quad (5)$$

where  $M_l^{sph}$  — mass of liquid contained at the spherical volume.

To determine the pulsator apparent mass, we must account that its presence at (3) is due to the medium resistance. Known is that in the sound source's near field, case of the propagating harmonic spherically symmetric wave, the acoustic resistance  $Z$  is determined by a complex expression:

$$Z = \text{Re} Z + \text{Im} Z = \rho_l c (kr^2) - i\rho_l ckr, \quad (6)$$

where  $r$  — radial coordinate;

$c$  — acoustic wave propagation velocity;

$k$  — wave number.

The expression (6) is valid under the  $kr \ll 1$  condition when the ratio between the real and imaginary impedance parts  $\frac{\text{Re} Z}{\text{Im} Z} = kr$  is small. Physically, this means that the active acoustic impedance and the associated energy dissipation during model pulsations are negligible. Considering the pulsator's near zone as an incompressible medium we can also neglect the elastic resistance, thus being limited in the impedance expression only with the resistance reactive component mass:  $Z = -i\rho_l ckr$ . From the viewpoint of mechanical representations the expression's negative character suggests that the medium mass reaction (as an external passive force) is applied directly to the pulsing volume.

At jet HDR operated in a liquid medium, the pulsing area radius is less than a centimeter at a wavelength of a meter order, so the equilibrium radius value in the studied pulsator model according to calculations based on (1), (2) does satisfy the condition  $kr_p \ll 1$ . Accordingly, the absolute value of the pulsator resistance reactive mass is given by:

$$\text{Im} Z \approx i\rho_l ckr_p = i\omega\rho_l R_p, \quad (7)$$

where  $\omega$  — pulse cyclic frequency.

In impedance expression (7) the value, determining the mass reactance to fluid pressure experienced by the pulsing area during vibration is  $\rho_l R_p$ . This value, in accordance with the unit  $\text{kg/m}^2$  takes the sense of mass surface density and characterizes the mass distribution by the pulsator surface depending on  $R_p$ . The larger is the surface the greater is the weight and the medium reactance, where-

by this last is called the mass resistance. Thus, for the entire closed pulsator surface the  $\int \rho_l R_p dS$  value is considered as a general integral characteristic of the medium mass reactance to the pulsator's fluctuations measured in units of mass and defined as an apparent mass.

In accordance with the above principle, for apparent mass of spherical pulsator we obtain, considering that  $R_p = \text{const}$  the following result, which coincides with the well-known equation:

$$M_a^{(1)} = S^{(1)} \rho_l R_p = 3V_p^{(1)} \rho_l = 3M_l^{sph} . \quad (8)$$

Joining (5) and (8) in compliance to (3) allows us to find the total mass for spherical pulsator model under first modification (re to Fig. 2, a):

$$M^{(1)} = (4 - \eta) V_p^{(1)} \rho_l = (4 - \eta) M_l^{sph} . \quad (9)$$

The same principle of determining the pulsator total mass can be used when considering the other pulsator geometric patterns. In particular, according to the considered HDR structure (Fig. 1), of interest is to reflect the volume of the nozzle-effluent jet occupying the central part of interflow area between the nozzle and the deflector. A corresponding sophisticated modification of the spherical pulsator model is shown in Fig. 2, b.

We shall consider the volume occupied by the nozzle-effluent jet, as an axial cylindrical channel, occupying a part of pulsator workspace. The HDR geometrical characteristics are such that the jet-occupied volume is comparable to this one of the pulsator work area. The surface of the flow channel in a pulsing cavitation zone is also the border of fluid-containing pulsator: a spherical pulsator in this modification has a kind of a "cut" inner cylindrical volume filled with the same liquid that is external to the pulsator area. Considering the "cut" jet amount in a straight circular cylinder with the height  $h = 2R_p$  and radius  $r_c$ , introducing the  $\beta = r_c/R_p$ , we obtain an expression for the pulsator equilibrium volume at this modification:

$$V_p^{(2)} = V_p^{sph} - V_p^c = V_p^{sph} \left( 1 - \frac{V_p^c}{V_p^{sph}} \right) = V_p^{sph} (1 - 1,5\beta^2) . \quad (10)$$

Then this modifications' pulsator own mass with respect to the expression (5) as above shall be written as:

$$M_c^{(2)} = (1 - \eta)(1 - 1,5\beta^2) M_l^{sph} . \quad (11)$$

Here the pulsator mass is expressed through the liquid mass  $M_l^{sph}$  contained in the full volume without "cut" area.

The apparent mass for a modified pulsator model, given the presence of the two surfaces, separating it from the external environment, consists of two components: the first representing the apparent mass, determined by the outer spherical surface and found in the previous case, according to (8), and the second being the mass added due to the inner cylindrical surface presence (apparent mass). We assume that it satisfies the  $r_c = \text{const}$  condition and the mass reactance is distributed over this surface evenly with a surface density  $\rho_l r_c$ . Then the second term for the apparent mass will be determined by the expression:

$$M_a^c = S^c \rho_l r_c = 2V_p^c \rho_l = 2M_l^c . \quad (12)$$

Thus, for the pulsator inner boundary the apparent mass is numerically equal to twice the weight of the liquid filling the cylinder's "cut" volume. Combining both terms, taking into account the expressions (8) and (12), we find the apparent mass for the pulsator spherical model second modification as follows:

$$M_a^{(2)} = M_a^{sph} + M_a^c = 3(1 + \beta^2) M_l^{sph} . \quad (13)$$

To get the total mass for the pulsator spherical model with cylindrical “cut” volume we summarize the (11) and (13):

$$M^{(2)} = M_c^{(2)} + M_a^{(2)} = M^{(1)} + 1,5(1 + \eta)\beta^2 M_l^{sph}. \quad (14)$$

The second term here represents a correction to the original pulsator’s spherical model total mass, taking into account the presence of a cylindrical channel.

**Results.** The studied theoretical material to determine the pulsing interflow area mass served in basis for calculating the total mass of pulsator spherical model in two versions for several counterflow HDR with characteristic deflectors dimensions of 2...5 mm. The pulsator equilibrium radius given in the model  $R_p$  was compared with the deflector parabolic concavity radius  $r_n$ . The size of pulsing area for each deflector may vary depending on the nozzle-to-deflector, distance so given radius defined for each HDR varied subject to the limitations imposed by the conditions (1) and (2). The model modification with a “cut” cylindrical channel considered the common to all studied HDR parameter: ratio between the radii of the nozzle (flow) and the deflector:  $r_c = 1/2 r_n$ .

The values adopted at calculations, were: density of water  $\rho_l = 1000 \text{ kg/m}^3$ ; gas share in the two-phase medium  $\eta = 0,388$  [1].

The pulsator total mass increases with increasing radius according to (9) and (14) by the cubic law. To assess the apparent mass contribution to the pulsator total mass there were compiled various relationships between the total mass and its components for various modifications of simple spherical pulsator model. In the original model, the ratio between total mass and the own weight of the pulsator:

$$\frac{M^{(1)}}{M_c^{(1)}} = 1 + \frac{M_a^{(1)}}{M_c^{(1)}} = 1 + \frac{3}{1 - \eta}.$$

Therefore, accounting the apparent mass we reach to observe an increase in total mass of the pulsator approximately 5,9 times. This value is constant for a given value of gas content. With increasing gas content the apparent mass contribution increases. A similar mass ratio is obtained for the modification with a “cut” cylinder:

$$\frac{M^{(2)}}{M_c^{(2)}} = 1 + \frac{M_a^{(2)}}{M_c^{(2)}} = 1 + \frac{3(1 + \beta^2)}{(1 - \eta)(1 - 1,5\beta^2)}.$$

As  $\beta = r_c/R_p$ , there is a dependence to the pulsator radius  $R_p$  (Fig. 3). The curves 1, 2, 3 are obtained for HDR with characteristic deflector dimensions (concavity radius) 2,5; 3,5; 5 mm, respectively. The jet radius is constant for every device, so at  $r_c \ll R_p$  the radius dependency is insignificant therefore possible is to use the simplest spherical model (when radius increase the mass ratio tends to reach the 5,9 constant). At pulsator radius decrease the apparent mass share increases. At  $r_c \approx R_p$  the cavitation area existence is impossible so for the “cut”-channel modification the condition  $R_p > r_c$  should be joined to (1) and (2), found for the initial variance of the spherical pulsator model and the small radii region should not be considered.

We also obtained the ratios of total and apparent masses for each of two modifications of the spherical model:

$$\frac{M^{(2)}}{M^{(1)}} = 1 + \frac{1,5(1 + \eta)}{4 - \eta} \beta^2; \quad \frac{M_a^{(2)}}{M_a^{(1)}} = 1 + \beta^2.$$

The mass ratio decreases with increasing radius of the pulsator (Fig. 4). The difference between the total mass of modifications in various models is low (except for small radii, which is not essential); when  $r_c \ll R_p$ , the mass of the pulsator in two versions are virtually identical. This is due to reduced influence of two factors: the own mass  $M_c^{(2)}$  decrease by reducing the pulsator volume that becomes more significant, with the cylinder radius increase, and a few more substantial increase in the apparent

mass. This is clearly seen from (11) and (13), where the values depending on  $\beta$  have different signs. Note that this effect has been observed for the spherical model of the pulsator; other models may give a different result; in each case, a separate study is needed.

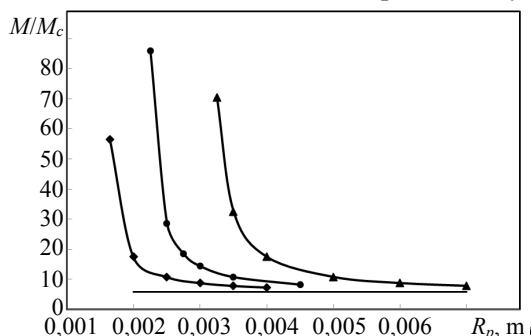


Fig. 3. Dependence of the ratio of pulsator's (2nd modification) total mass to its own mass on its radius for HDR with such deflector's radii: 1 — 2,5 mm (rhomb); 2 — 3,5 mm (circle); 3 — 5 mm (triangle)

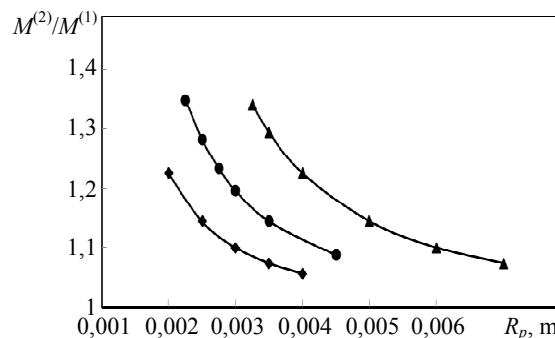


Fig. 4. Dependence of the ratio of pulsator's total masses in both modifications on its radius for HDR with such deflector's radii: 1 — 2,5 mm (rhomb); 2 — 3,5 mm (circle); 3 — 5 mm (triangle)

The results of calculations of the pulsator masses ratio and their modifications for the two characteristic HDR dimensions are shown in Table 1.

Table 1

The dependence of the mass ratios' relation, case of the pulsator spherical model modifications, from its radius at different HDR deflector radii

Deflector radius, mm					Deflector radius, mm				
2,5					5,0				
Pulsator radius, mm	$\frac{M^{(2)}}{M_c^{(2)}}$	$\frac{M_a^{(2)}}{M_c^{(2)}}$	$\frac{M^{(2)}}{M^{(1)}}$	$\frac{M_a^{(2)}}{M_a^{(1)}}$	Pulsator radius, mm	$\frac{M^{(2)}}{M_c^{(2)}}$	$\frac{M_a^{(2)}}{M_c^{(2)}}$	$\frac{M^{(2)}}{M^{(1)}}$	$\frac{M_a^{(2)}}{M_a^{(1)}}$
1,65	56,46	55,46	1,33	1,57	3,25	70,40	69,40	1,34	1,59
2,0	17,46	16,46	1,23	1,39	3,5	32,54	31,54	1,29	1,51
2,5	10,80	9,80	1,14	1,25	4,0	17,46	16,46	1,22	1,39
3,0	8,78	7,78	1,10	1,17	5,0	10,80	9,8	1,14	1,25
3,5	7,83	6,83	1,07	1,12	6,0	8,78	7,78	1,10	1,17
4,0	7,30	6,30	1,05	1,10	7,0	7,83	6,83	1,07	1,12

**Conclusions.** Determination of the mass ratio allows us to estimate the apparent mass' effect to the inertial properties of the studied pulsator. Such assessment provides possibility in each case to take into account (or ignore) the mass reactance forces effect onto fluctuations in the fluid of the given material object. An important role in determining the mass ratios is attributed to the characteristic dimensions of both the pulsator and the counterflow interflow HDR area. Just the area geometry determines the specifics of pulsator modeling. The relationship of mass can be also considered in a similar manner for other models with regard to their geometric features. A comparison of the different simulative versions with varying the area's geometric parameters allows optimizing the effect of the pulsator inertial properties in whole and as to its apparent mass, in particular when solving research problems of HDR acoustic features. This is the main prospect of further researches as to inertial properties of pulsing interflow area as an integral part of the system, representing the source of acoustic emission at HDR.

Analyzing the study results allows to establish the following:

— When assessing the counterflow HDR pulsing interflow area inertial properties a predominant role is tribute to the apparent mass, which is almost 6 times more than the own mass of the pulsator.

The resulting mass ratio show that the apparent mass effect increases with increasing gas content of the two-phase medium, i.e., the cavitation progress.

— Accounting for simple spherical model the central axial channel occupied by the nozzle-effluent jet, even more evidently shows the contribution of the apparent mass in the total mass of the pulsator. At small values of the pulsator radius its own mass in comparison with the apparent one can be neglected.

— The total mass of pulsing area in two spherical model versions are close to each other due to the mutual compensation of two factors: the pulsator apparent mass growth and its own mass reduced at a relatively small volume of a sphere.

### Література

1. Вовк, И.В. О возможном механизме автоколебаний в струйных гидродинамических излучателях с развитой кавитацией / И.В. Вовк, В.Т. Гринченко, Ю.М. Дудзинский // *Акуст. вісн.* — 2008. — Т. 11, № 2. — С. 16 — 23.
2. Дудзинский, Ю.М. Модель поперечных колебаний затопленных струйных оболочек / Ю.М. Дудзинский, В.В. Витков, А.В. Жукова // *Пробл. обчисл. механіки і міцності конструкцій.* — 2011. — Вип. 15. — С. 93 — 99.
3. Дудзинский, Ю.М. Свойства кавитационной области струйного гидродинамического излучателя в условиях гидростатического давления / Ю.М. Дудзинский, А.В. Жукова // *Акуст. вісн.* — 2009. — Т. 12, № 3. — С. 27 — 32.
4. A model of acoustic transmission in the respiratory system / G.R. Wodicka, K.N. Stevens, H.L. Golub, etc. // *IEEE Transactions on Biomedical Engineering.* — 1989. — Vol. 36, Issue 9. — PP.925 — 934.

### References

1. Vovk, I.V., Grinchenko, V.T., & Dudzinskii, Yu.M. (2008). On possible self-oscillation mechanism in hydrodynamic jet radiators with developed cavitation. *Acoustic Bulletin*, 11(2), 16–23.
2. Dudzinsky, Yu.M., Vitkov, V.V., & Zhukova, A.V. (2011). Model of transversal vibrations of the flooded jet shells. *Problems of Computational Mechanics and Strength of Structures*, 15, 93–99.
3. Dudzinskii, Yu.M., & Zhukova, A.V. (2009). Properties of the cavitation zone of a jet hydrodynamic radiator in conditions of excessive hydrostatic pressure. *Acoustic Bulletin*, 12(3), 27–32.
4. Wodicka, G.R., Stevens, K.N., Golub, H.L., Cravalho, E.G., & Shannon, D.C. (1989). A model of acoustic transmission in the respiratory system. *IEEE Transactions on Biomedical Engineering*, 36(9), 925-934. DOI:10.1109/10.35301

Received July 22, 2015

Accepted October 10, 2015